EVALUATION OF CO₂, CH₄, AND O₃ GHGs FROM SATELLITES AGAINST GROUND-BASED MEASUREMENTS OVER SULAIMANI City, KR, IRAQ

W. J. Abdlrahman¹

P. M. Najmaddin¹

S. N. Majid¹

Researcher

Assist. Prof.

Assist. Prof.

¹ Dep. Natural Resources -Coll. Agric. Engine. Sci. University of Sulaimani

E-mail: wanawsha.abdlrahman@univsul.edu.iq

ABSTRACT

This study was conducted from December 2021 to July 2022, except May 2022, and aimed to evaluate and validate CO₂, CH₄, and O₃ GHGs in 13 different locations over Sulaimani city, Kurdistan Region-Iraq by means of remote sensing techniques from Sentinel 5 Precursor (S5P)/ TROPOMI and Orbiting Carbon Observatory-2 (OCO-2) satellites against ground-based measurements by using a portable gases analyzer via three types of sensor heads, GSS for the nominated gases of CO₂, CH₄, and O₃. The Inverse Distance Weight (IDW) interpolation methods were used to map the CO₂, CH₄, and O₃. The results of ground measurements showed high variability in some greenhouse gas concentration values and ranged between 285-508 ppm, 0-17000 ppb, and 0.25-64 ppb for CO₂, CH₄, and O₃, respectively, in different locations and months. Satellite-predicted values for CO₂, CH₄, and O₃ ranged between 416 - 418 ppm, 1858.99 - 1908.26, and 15.13 - 16.96 ppb, respectively, among the studied locations during the study periods. The RMSE ranged between 0.5 - 92.75 ppm, 99.11 – 2593.05 ppb, and 0.08 – 48.87 ppb for CO₂, CH₄, and O₃, respectively.

Keywords: greenhouse gases, satellite remote sensing, validation, ground measurement.

عبدالرحمن وآخرون

مجلة العلوم الزراعية العراقية- 2025: 56 (5):1747-1763

تقييم مستوى الغازات الدفيئة من ثاني أكسيد الكربون، الميثان والأوزون من الاقمار الصناعية

مقابل القياسات الأرضية في مدينة السليمانية ، كردستان ، العراق

صالح نجيب مجيد

پيشهوا مصطفي نجم الدين

وهنهوشه جمال عبدالرحمن

أستاذ مساعد

أستاذ مساعد

باحث

قسم الموارد الطبيعية – كلية علوم الهندسة الزراعية – جامعة السليمانية

المستخلص

أجريت هذه الدراسة في الفترة من كانون الثاني 2021 إلى تموز 2022، باستثناء أيار 2022 لغرض التحقق من صحة تراكيز الغازات الدفيئة ($_{03}$ 0 CH₄0 و $_{03}$ 0 CH₈0 كن بعد من الاقمار الصناعية : ($_{03}$ 0 CH₉0 CO₀0 CH₉0 Precursor (SSP) and Orbiting Carbon Observatory-2 (OCO-2) عن بعد من الاقمار الصناعية : $_{03}$ 0 CH₉0 CO₀0 April CO₀0 A

الكلمات المفتاحية: غازات الاحتياس الحراري، الاستشعار عن بعد بالساتل ، تصديق، قياسات أرضية



This work is licensed under a Creative Commons Attribution 4.0 International License. Copyright© 2025 College of Agricultural Engineering Sciences - University of Baghdad

Received: 27/12/2022, Accepted: 29/3/2023, Published: October 2025

INTRODUCTION

The natural phenomenon of greenhouse effect allows our planet to sustain life and maintain the necessary conditions to harbor life. But, the main cause of climate change is the increase of atmospheric concentration for the natural greenhouse gases (GHGs) of carbon dioxide (CO₂), Methane (CH₄), Nitrous oxide N₂O, Ozone (O₃), and water vapor H₂O as well to synthetic chemical compound of greenhouse gases, such as; hydrofluorocarbons (HFCs), perfluorocarbons (PFCs), Sulfur hexafluoride (SF6), and Nitrogen trifluoride (36). The changes in climate that can be attributed to continuing releases of GHGs could have large detrimental impacts on human safety and well-Accordingly, there have being. been international efforts reduce to **GHGs** productions by many countries through setting legally binding targets for reductions GHGs and particularly CO₂ gas over coming decades (16). GHGs have the ability to absorb infrared radiation (IR) reflected by Earth's surface, clouds, and atmosphere, conversely, if it is not absorbed by the GHGs, it would be directed to the space. The absorption and re-emission of infrared radiation by GHGs could warms Earth's lower atmosphere and also earth surface, and this process is known by "Greenhouse Effect." Increasing of GHGs by anthropogenic activities released enhancing the Greenhouse Effect, and it is the crucial cause of climate change (17). Despite the uptake of a large portion of GHGs emissions by various natural " sinks" which involved in Carbon cycle, burning fossil fuels has contributed to a 40% increase in concentration of Carbon dioxide atmosphere, and this increased concentration of CO₂ from 280 to 397 ppm since the beginning of Industrial Revolution. GHG emissions from human activities (anthropogenic) alter the Earth's energy balance between incoming solar radiation and heat expelled back into space, resulting in climate change (1). CO₂ concentration in atmosphere recorded at the Mauna Loa laboratory in October 2022 was 415.78 ppm, while it was 280 ppm during the preindustrial times. Consequently, the average global surface temperature has risen by 0.85 Celsius degrees since pre-industrial times (15). CO₂ has risen dramatically, and that increase in concentration is due to factors of deforestation, land-use change, cement manufacturing, and fossil fuel burning, which became the primary source of emissions in 1950s (7). CO₂ is considered as basic contributor to radiative forcing of Earth planet, which leads to climate change, while the succeeding contributors are CH₄ and N₂O. Likewise to CO₂, there still is large doubt on the sources of CH₄ and N₂O in the atmosphere (5). The in-situ and ground measurement technique is used to display surface concentrations of atmospheric GHGs (24,38). Also, several satellites and remote sensing techniques can be used to measure atmospheric concentration of GHGs. Normally, remote sensing satellite imagery is more specific and delivers more data than simple images (14). Satellites technology have distinctive ability to provide global coverage Earth's surface and atmospheric composition that is not possible by using ground-based monitoring techniques or to assess the impact of urbanization growth on climate (25). As a result, our understanding of Earth and its key systems has improved significantly since the launch of observation satellites in the 1960s (16). GHGs differ in their global warming potential (GWP) or capacity to absorb energy, this means that they have different radiative efficiencies. Also, they differ in their atmospheric lifetime or residence times. Therefore, this study was conducted during December 2021 to July 2022 and aimed to evaluate and validate of CO₂, CH₄, and O₃ GHGs in 13 different locations over Sulaimani city, Kurdistan Region-Iraq by means of remote sensing techniques from Sentinel 5 Precursor (S5P)/ TROPOMI and Orbiting Carbon Observatory-2 (OCO-2) satellites against ground-based measurements. Finally, ArcGIS 10.8 program was used for mapping, validation, and interpolation. Also, the study is aimed to improve monitoring and environmental services management Kurdistan region. However, hindrances and complications that faced our study were the lack of a monitoring station as well as the shortage of background data concerning GHGs.

MATERIALS AND METHODS

Study areas: This research study was conducted in Sulaimani (Sulaymaniyah) City in Kurdistan region-Iraq, which is located by the Latitude and longitude coordinates of; 35°33'53" N and 45°25'58" E, respectively. Moreover, the study area's altitude ranged between 671 m to 1098 m Figure 1. Sulaimani Governorate is located in the east of Iraq's Kurdistan Region, not far from Iran-Iraq border (2), and has an area of about 18822 km², altitude of about 882 m, and the population is more than 1,783,270 (41). However, the climate of study area is hot and dry over summer season, while it is cold in winter seasons. Nonetheless, the annual precipitation average ranges from 450 to 700 mm (30).

Ground measurements

Based on population density, traffic intensity, pollution sources such as car exhausts and factory residues, and other human activities, thirteen sites (13 locations) were selected for this study to cover all the city's area Table 1. Ground spatial and temporal data on three GHGs (CO₂, CH₄, and O₃) concentrations were measured weekly from December 2021 to July 2022, except May 2022 because portable gas analyzermodel Series 500 sent maintenance and calibration, by using a New Zealand product of portable gas analyzermodel Series 500 - Portable Air Quality Monitor via three types of sensor heads, GSS (gas-sensitive semiconductor) nominated gases of CO₂, CH₄, and O₃. Measurements were conducted 23 times throughout the period from 11/12/2021 to 7/7/2022. The unit of concentrations measurement was in parts per million (ppm) for CO2 gas, while for CH4 and O3 were in parts per billion (ppb). The Ground measurements were then compared to remote sensing data. Carbon dioxide (CO₂) data was obtained from Orbiting Carbon Observatory-2 (OCO-2) satellite. Methane (CH_4) Ozone(O₃) data were obtained from Sentinel 5 Precursor TROPOMI (S5P) satellite. Finally, ArcGIS 10.8 program was used for satellite maps, validation, and interpolation. Validation are techniques used to assess how well an interpolation model performs.

The attained Satellite data or satellite imagery data for CO_2 and CH_4 concentrations was in mol/mol unit and then converted to ppm and ppb, respectively. However, the obtained Satellite data of O_3 concentration was in mol/m^2 and then converted to ppb.

Interpolation methods

The current study used the inverse distance weighted (IDW) method for interpolation procedure to visualize and analyze the spatial inconsistency and temporal dynamics of atmospheric GHGs of CO₂, CH₄, and O₃ concentrations because IDW has been widely used in contamination mapping, weather analysis, hydrological analysis, and so on (27). IDW is a deterministic spatial interpolation approach for points near together and is more alike than those farther apart. Accordingly, a location's concentration may be predicted by adding the weighted concentrations of other known places (28).

Validation

The Split-data-sets-validation approach was used to evaluate the effectiveness of spatial interpolation technique. It involves splitting points into two groups: points used in interpolation operation and points needed to verify the findings (29). In this research, 6 points were selected randomly for validation and 7 points for interpolation operation in 13 points for each month. Two statistical metrics were used for validation, firstly is, the rootmean-square error (RMSE), as shown in Equation (1), and secondly is, the percent bias (Equation 2).

$$RMSE = \sqrt{\frac{\sum_{i=1}^{n} (Xi^{RS} - Xi^G)^2}{N}}$$
 (1)

Percent bias =
$$\frac{\sum_{i=1}^{N} (Xi^{RS} - Xi^G)}{\sum_{i=1}^{N} Xi^G} \times 100 \quad (2)$$

Where X_i^G and X_i^{RS} are the ground and RS values, respectively, and N is the number of values recorded.

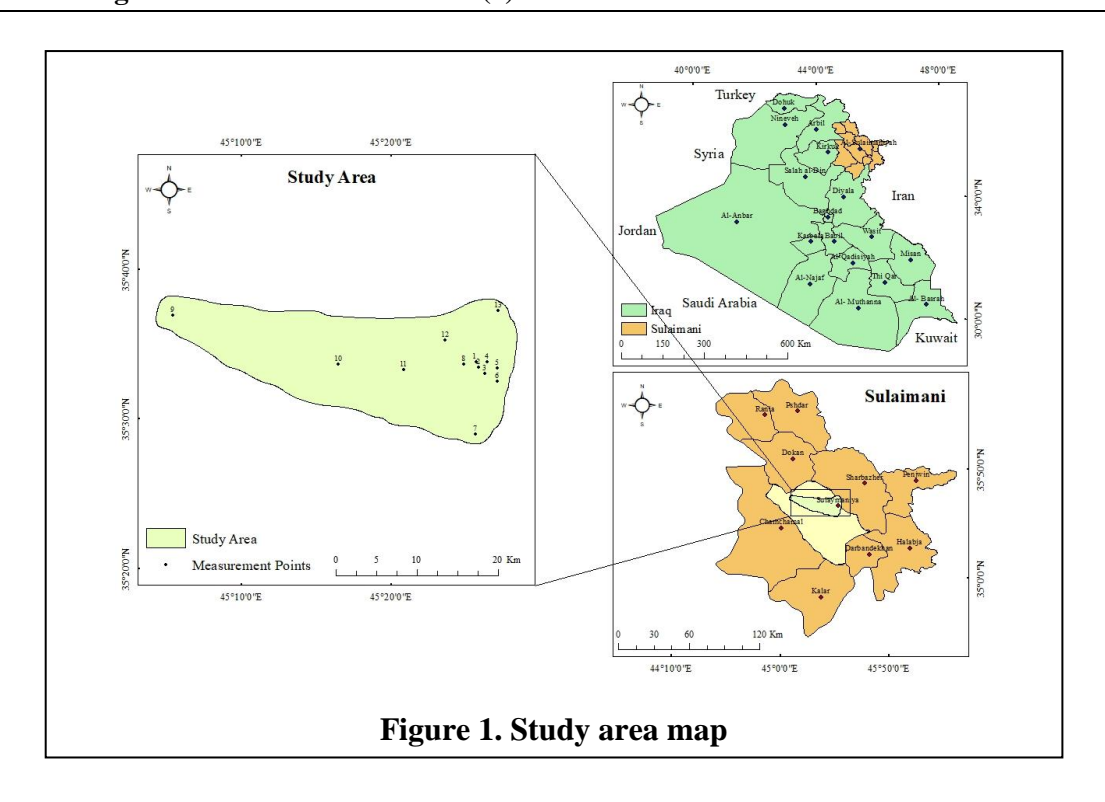


Table 1. Location name, latitude, longitude, and altitude in meter (m)

Location Numbers	Location Names	Latitude	Longitude	Altitude (m)
1	Civil Development Organization (C.D.O)	35.56302778	45.42727778	844
2	Salimstreet(cigarettecargo)	35.55683333	45.43055556	846
3	Dastaraka	35.55002778	45.43738889	836
4	Qanatstreet	35.56308333	45.43994444	874
5	Brimpashastreet	35.55605556	45.45091667	875
6	Qrga	35.54163889	45.45072222	869
7	Tanjaro	35.48277778	45.42652778	671
8	Salimstreet(hajehasanyloka)	35.56097222	45.41338889	808
9	Bazyan	35.61494444	45.09091667	832
10	Kelaspy	35.56066667	45.2745	759
11	Bakrajo	35.55447222	45.34736111	744
12	Sarchnar	35.58736111	45.39333333	800
13	Hawareshar Park	35.62080556	45.45161111	1098

RESULTS AND DISCUSSIONS

Ground measurements of CO_2 , CH_4 , and O_3 concentration in ppm and ppb Carbon dioxide (CO_2)

Carbon dioxide (CO₂) is a trace gas of the atmosphere, in 1958, atmospheric CO₂ at Mauna Loa was about 320 parts per million (ppm), but it was in November 2022, for globally averaged concentration approximately of 417.51 ppm was documented in the Earth's atmosphere by Mauna Loa observatory/Hawaii (31), and certainly, this varies spatially and temporally. As shown in Table 2, CO₂ results showed high variability in concentration values among the 13 studied locations, and temporal differences between minimum and

maximum levels of ground CO₂ concentration values among the locations were ranged between (411.5-508.8); (417.5-504); (374.8-448.8); (337.5-377); (285.0-408.0); (427.8-491.8); and (430-466) ppm along the month of Dec./2021 as well as the months of Jan., Feb., Mar., Apr., June, and July/2022 respectively. The minimum value of 285.0 ppm was found at location 13 in April 2022, while the maximum value of (508.75) ppm was found at location 8 in December 2021. Location 8 is in the center of Sulaimani city and considered as one of the hotspots of urban area in Sulaimani city due to the fact that location 8 is characterized by a large and dense car traffic. While locatio13 is a large garden and includes

a large number of different plants, thus the process of photosynthesis is efficient in maintaining the balance of oxygen and carbon dioxide. Besides, the minimum difference value of range among locations was 36 ppm and found in July/ 2022, while maximum difference value of the range among locations was 123 ppm and revealed in April /2022. This might be attributed to the facts that there are many different factors that influence the rate of CO₂ production in a local place, and these factors are like; population growth, economic growth. amount of fossil fuel energy consumption, changing energy prices, using technologies in industrialization, new changing in human behavior, urbanization, and seasonal temperatures (23). It is worth noting that the average measured concentration of carbon dioxide in the following locations 1, 2, 3, 4, 5, 8, and 11 was higher than the global average measured in November, which was (417.51 ppm) by (31), and this indicates that the sources of carbon dioxide emission are more or might be more emitted. However, in comparison to these outcome of CO₂ by current study, the author Majid (26) found a wider concentration range of 371 – 1159 ppm when the author measured the concentration of CO₂ in ambient air for seven 7 times and during measuring period from 31.9.2009 to 13.7.2010 at 17 different location in Sulaimani city, the higher average concentration level by author was found inside Peshraw tunnel, and that was due the passage of a large number of cars inside tunnel with a length of 2.5 km as well as a shortage of ventilation system. In general, it is well known that CO₂ is added to atmosphere naturally from different sources like organisms respiration, organic matter decomposition (decay), wildfires or forest fires occurring, carbonate rocks weathering, volcanic eruption, car exhausts and factory waste. It is also noteworthy that all minimum levels during seven 7 months of study were appeared at location13 or Hawareshar park, which is a large public garden and planted by various plants that act as CO₂ sinks. However, the descending order of average CO₂ concentration levels among the months of study was as follows: 463.35> 462.35 > 458.52 > 447.37 > 414.63 > 362.10 > 333.13 for the months Jan./22, Dec./21, Jun./22, Jul./22, Feb./22, Mar./22, and Apr./22 respectively. High average level of CO2 in Jan./22 and Dec./21 can be attributed to fact that in winter, hemisphere is tilted away from the sun, thus hemisphere get less direct sunlight and temperatures just for fewer hours per day which at the end play a vital role for photosynthesis process in plant leaves and then carbon phytosequestration or storing it in Accordingly. wood. this causes hemisphere to get less direct sunlight in fewer hours of a day and temperatures. Moreover, deciduous trees have a seasonal carbon dioxide exchange pattern that is lead to sink or reduce less atmospheric carbon dioxide in winter season because, at end of autumn season, deciduous trees mostly lose their leaves for next season of winter (9,35). Generally, the average descending order concentrations among the locations showed the following sequence; 448.69> 439.37> 431.42> 431.23> 425.18> 420.56> 418.24> 415.90> 414.38 414.38> 415.14> 403.82>383.44 for the location numbers; 8, 4, 1, 2, 5, 11, 3, 7, 6, 9, 12, 10, and 13.

Table 2. The concentrations of CO₂ (ppm), CH₄(ppb), and O₃(ppb) for the studied location from December 2021 to July 2022

Location Number	Gases	December	January	February		April	June	July	Average Values
	CO ₂	469.5	467.5	416.16	372.5	385	461.25	448	431.42
1	CH_4	1250	750	500	1500	17000	1750	3500	3750.00
	O_3	2.5	9.75	23.33	19.5	7	18.25	43.5	17.69
	CO_2	455.75	486.25	419.83	377	360	453.75	466	431.23
2	CH_4	2250	750	500	1500	13000	750	2500	3035.71
	O_3	6.75	13	32.5	35	23	29	25.5	23.54
	CO_2	449.5	468	411.16	362.5	343	451.5	442	418.24
3	CH_4	3250	1250	1166.66	1500	16000	500	3500	3880.95
	O_3	12.5	11	32.5	37	33	24.75	25.5	25.18
	CO_2	475	500.5	448.83	364	347	491.75	448.5	439.37
4	CH_4	4250	3250	2666.66	3000	3000	1000	4500	3095.24
	O_3	0.75	3.75	10.83	10.5	3	2.5	31.5	8.98
	CO_2	461.75	467.75	429.5	377	315	469.25	456	425.18
5	CH_4	3500	1750	1500	2500	1000	3500	4000	2535.71
	O_3	0.25	4.75	11	14.5	12	12	17	10.21
	CO_2	446.25	443.25	420.5	374	294	482.5	445.5	415.14
6	CH_4	3750	1000	1000	1000	0	1500	3500	1678.57
	O_3	6	16.75	15	12	16	8.75	21	13.64
	CO_2	472.25	442.5	407.83	360	299	470.75	459	415.90
7	CH_4	1500	500	1000	1500	0	750	4500	1392.86
	O_3	21.25	35.75	37.66	38.5	45	29.75	38	35.13
	CO_2	508.75	504	448.33	362.5	408	458.75	450.5	448.69
8	CH_4	2250	250	500	0	14000	1500	3500	3142.86
	O_3	6	11	18.33	26.5	1	31.5	24.5	16.98
	CO_2	466	458.33	409.83	347	341	445.5	433	414.38
9	CH_4	500	1000	833.33	0	5000	500	3000	1547.62
	O_3	14.5	18.75	33.83	51	20	50	49.5	33.94
	CO_2	447.75	446.75	395	342	314	440.75	440.5	403.82
10	CH_4	1500	1750	1166.66	0	1000	1000	2500	1273.81
	O_3	22.25	29.25	44.33	53	41	58.5	61	44.19
	CO_2	459.25	468	415.66	371.5	320	455.5	454	420.56
11	CH_4	2000	500	1000	500	0	1250	2000	1035.71
	O_3	9.5	18	30.5	31.5	26	32	30.5	25.43
	CO_2	491.25	458.25	398.5	369.5	293	448.75	441.5	414.39
12	CH_4	1000	500	1000	500	0	1250	2000	892.86
	O_3	5	17.75	28.16	37.5	36	39.75	36	28.59
	CO_2	411.5	417.5	374.83	337.5	285	427.75	430	383.44
13	CH_4	1250	0	0	0	0	1750	500	500.00
	O_3	16.25	28.5	36.16	60	54	46.25	64	43.59

Methane (CH₄)

Methane (CH₄) is also a trace gas of atmosphere, in 1984, atmospheric methane concentration at Mauna Loa was about 1644.69 parts per billion (ppb), but it was in August 2022, for a globally averaged concentration of approximately of 1908.61 ppb documented in Earth's atmosphere via Mauna Loa observatory/Hawaii (31), and certainly, it varies temporally and spatially. As revealed in Table 2, a great variation for the temporal differences between minimum and maximum levels of ground CH₄ concentration values

were found and ranged between (500-4250); (0.0-3250); (0.0-2666.7); (0.0-3000); (0.0-17000); (500-3500); and (500-4500) ppb along the month of Dec./2021 as well as the months of Jan., Feb., Mar., Apr., June, and July/2022 respectively. The lowest value of zero (0.0) was found in more than one location, such as location 13, in January, February, March, and April 2022. Also, at locations of 8, 9, and 10 in March. However, at location 6, 7, 11, and 12, zero emission level was occurred in April. In contrast, the highest value of (17000) ppb was found in April at location 1 because it is

regarded as one of the most urban hot spots areas within Sulaimani due to its heavy traffic condition. Temporal and spatial zero level concentration of atmospheric methane in some of studied locations might be either due to limited sources of CH₄ emission or to fact that nearly ninety percent (90%) of CH₄ is removed by the reaction process of photooxidation (13). However, the minimum difference value of range for CH₄ among locations was 2666.7 ppb and occurred in Feb.2022, while maximum difference value of range among locations was 17000 ppb and appeared in April 2022. In General, many sources and particularly anthropogenic activities contribute in CH₄ emissions like; agricultural activities, landfills, wastewater treatment, oil and natural gas systems, coal mining, certain industrial processes, stationary and mobile combustion (11). Certainly, the sources of methane emission differ in locations and among months of study in terms of presence and the amount of emission inevitably, their instantaneous SO concentrations vary when measured. It should be pointed out at the locations 1, 2, 3, 4, 5, and 8 that the maximum temporally concentration of CH₄ has exceeded globally averaged concentration of approximately of 1908.61 ppb at Mauna Loa Observatory/ on island of Hawaii (31), and this can be attributed to fact over last two centuries, concentrations in atmosphere have more than doubled CH₄ concentration, mostly due to anthropogenic activities (11). Also, location feature in Sulaimani is defined by rural, urban, and urban hot areas, and this cause a significant variation of CH₄ concentration. Therefore, high concentrations of CH₄ were recorded in hot spot locations where human activity and traffic vehicles lead to significant emissions of CH₄ throughout the streets. Additionally, Methane results showed a seasonal fluctuation, and maximum CH₄ concentrations were recorded in April, June, and July 2022 (Table 5). The maximum level of CH₄ were recurrent five times at location 4 during the months of Dec./2021, then Jan., Feb., Mar., Apr., and Jul./2022. This might be caused by more dense traffic or running of heavy traffic on Qanat-street. But, the minimum level were repeated five times at location 13 (Hawareshar park) and twice at location 9 (Bazyan), and both locations are non-urban area, therefore, they were less polluted with atmospheric CH₄ gas. On the other hand, the descending order of the average CH₄ concentration levels among the months of study was as follows: 5384.6> 3038.5> 2173.1>1307.7 > 1038.5 >1019.2 >987.2 ppb for the months: Apr./22, Jul./22 Dec./21, Jun/22, Mar./22, Jan./22, and Feb./22. And when comparing our results for atmospheric CH₄ gas with average of what is indicated by NOAA (31), we find that some of our ground measurements are much higher because NOAA has stated that atmospheric CH₄ concentration has continued to increase since 2011 to an average global concentration of 1895.3 ± 0.6 ppb as of 2021. Also, NOAA showed that the May 2021 peak was 1891.6 ppb, while the April 2022 peak was 1909.6 ppb, and this means an increase of 0.9% from the May peak of 2021 to the April peak of 2022, and this can be ascribed to the fact of differences between our ground and RS measurements by NOAA, and also to fact that NOAA measurements were conducted at a oceanic location. Generally, remote descending order of average CH_4 concentrations among the locations showed the following sequence; 3880.95> 3750.00> 3142.86> 3095.24> 3035.71> 2535.71> 1678.57> 1547.62> 1392.86> 1273.81> 1035.71> 892.86>500.00 for location numbers; 3, 1, 8, 4, 2, 5, 6, 9, 7, 10, 11, 12, 13 respectively. It is noted that there are observable or sometimes differences between the locations regarding the concentration of CH₄. This may be due to the different characteristics of locations for the emission of CH₄. of the aforementioned about Carbon dioxide and Methane, it is important to mention that CO₂, CH₄, as well as N₂O, are long-lived greenhouse gases because they are chemically stable and continue to existent in atmosphere over time scales of a decade to centuries or longer, thus that their existences have a long-term influence on climate change (18).

Ozone (O₃)

According to Americans Children and the Environment (3), O₃ is regarded as one of six 6 collective air pollutants recognized in Clean

Act. EPA calls these "criteria air pollutants" because their levels in outdoor air need to be limited or restricted grounded on health criteria. Moreover, unlike other criteria air pollutants, O₃ is not emitted directly by any one of anthropogenic or natural sources. As shown in Tables 4 and 5, and also likewise CH₄, a significant variation for the temporal differences between minimum and maximum levels of ground O₃ concentration values were distinguished and ranged between (0.25-22.25); (3.75-35.75); (10.83-44.33); (10.5-60.0); (1.0-54); (2.5-58.50); and (17-64) ppb along month of Dec./2021 as well as months of Jan., Feb., Mar., Apr., June, and July/2022 respectively. The minimum concentration limit of (0.25) ppb was found at location 5 in December 2021, while the highest O_3 concentration of (64.0) ppb was recorded at location 13 in July 2022, which is considered as a nonurban area or, rather, it is a garden with a large plant intensity or high vegetation cover and the other reason is the presence of winds and their directions from Sulaymaniyah to Hawarishar park. Furthermore, all the concentration levels of O₃ concentration in this study were less than 70 ppb of EPA (11) air quality standard, or they were within the acceptable limits of air quality. On the other hand, and in comparison to these outcomes of O₃ in this study, Majid (26) found a wider concentration range of 26 -125 ppb when the author measured the concentration of ozone in ambient air for seven 7 times and during measuring period from 31.9.2009 to 13.7.2010 at 17 different location in Sulaimani city, higher average concentration level by author (26) was found inside Peshraw tunnel, and that was due the passage of a large number of cars inside the tunnel with a length of 2.5 km as well as a shortage of ventilation system. While the lowest average level was detected at location 8 (outside the Peshraw tunnel by 50 meters). On the other hand, the minimum difference value of the range for O₃ among the locations was 22.0 ppb and occurred in Dec.2021, while the maximum difference value of the range among locations was 56 ppb and revealed in June 2022. The results of O₃ concentrations showed an increasing trend with increasing atmospheric temperature and solar radiation. It is observable that high

concentration values of O3 were recorded in summer season and during daytime when was Still, sunlight intense. high concentrations were recorded in areas with high vegetation cover, this can attributed to the fact that trees affect the atmospheric O₃ concentration through emission of biogenic volatile organic compounds (BVOC), which can act as a precursor of O₃ formation as well as by its deposition on leaves (12). Also, the role of urban trees with regard to O₃ concentration will get further importance as nitrogen oxides (NOx) concentrations continue and climate decreasing warming progressing-rendering, especially when the urban ozone chemistry more sensitive to biogenic volatile organic compounds (BVOC) emissions. Nevertheless, the role of urban vegetation on local regulation of tropospheric O₃ concentrations is complex and largely affected or controlled by species-specific emission rates of BVOCs and O₃ deposition rates, and they are (both BVOCs and O3 deposition rates) highly altered by physiological status of trees (12).mentioned previously, tropospheric O₃ is an important secondary pollutant and also plays a atmospheric key role in chemistry. Tropospheric O₃ is produced by a series of complex photochemical reactions from its precursor gases, including nitrogen oxides (NOx) and non-volatile organic compounds (NVOCs), which are emitted by automobile tailpipes and smokestacks with the aid solar irradiation (20,40). Additionally, the emission and dynamics extremes of tropospheric O₃ and its natural precursors are impacted by climatic changes (8). The researcher Li, Jacob (22) has pointed out that longer period of air stagnation and higher temperature in future may lead to an increased O₃ concentration level. Moreover, according to Sekiya and Sudo (39), increasing water vapor and precipitation due to climate change are expected to reduce concentration. The maximum concentration levels of O₃ were recurrent three times at location 10 (Kelaspy) during the months of Dec./2021, then Feb., and Jul./2022. Furthermore, maximum level of O₃ were also three times at location recurrent (Hawaeshar Park) during months of Mar., Apr., and July 2021. This may be due to fact that two locations are regarded as rural locations with little vehicle traffic of main source of nitrous oxide N₂O emission, which play a vital role to Ozone depletion. Accordingly, the Ozone level remains at a higher concentration in remote areas compared to areas with heavy traffic. However, the minimum concentration levels of O₃ were mostly recurrent at location 4 Qanat street (four times) and location 5 Brimpasha street times), and both locations characterized by lack of vegetation cover, but the presence of heavy vehicles in traffic, which is the main source of N₂O emissions for O₃ decomposition (34). In general, the average descending order of ground O₃ concentrations among locations showed the following sequence; 44.19> 43.59 >35.13 > 33.94 > 28.59 > 25.43 > 25.18 > 23.54 > 17.69 >16.98> 13.64 > 12.21 >8.98 for location numbers; 10, 13, 7, 9, 12, 11, 3, 2, 1, 8, 6, 5, 4, respectively. It is noted that there are observable or sometimes significant differences between the locations regarding the average concentrations of O₃. This may be

due to the different characteristics of locations for emission of O₃ gas. And on the other hand, descending order of ground O₃ concentrations during months of study showed the following 35.96> 32.81>29.46>27.24> sequence; 24.46>16.76>9.5 for the months of July, March, June, Feb, April, Jan/22, December/21, respectively. It is revealed that higher concentrations of detected Ozone were occurred mostly by hottest and sunniest months. Normally, the high concentrations level of ground O₃ gas may disturb the ecological environment, growth of plants and animals as well as public health. Also, O₃ absorbs solar spectrum of ultraviolet radiation, and then leading to global warming, climate change, and then affects the ecological balance (6).

Assessment of Inverse Distance Weighting (IDW) Interpolation

The proposed method was applied for CO_2 , CH_4 , and O_3 concentrations calculation in this section and for each month of studying separately.

Table 3. Accuracy assessment of interpolation (IDW) method

Cassas	December				January		February		March		April		J	une	July	
Gases	IDW-R2	IDW-Slop	IDW-R2	IDW-Slop	IDW-R2	IDW-Slop	IDW-R2	IDW-Slop	IDW-R2	IDW-Slop	IDW-R2	IDW-Slop	IDW-R2	IDW-Slop		
CO2	0.47	0.0757x	0.04	0.0437x	0	0.0422x	0.02	0.1181x	0.57	0.4417x	0.21	0.1377x	0.28	0.2077x		
CH4	0.69	0.5713x	0.18	0.1065x	0.2	0.1382x	0.23	0.2235x	0.57	0.4777x	0.0013	0.0439x	0.48	0.3069x		
03	0.11	0.2718x	0.24	0.4454x	0.21	0.2529x	0.1	0.201x	0.06	0.1669x	0.33	0.3635x	0.17	0.8007x		

Table 3 shows the weight values for CO₂ of IDWr² and IDW-slope ranged between 0.02 to 0.57 and 0.0422 0.4417, respectively, during seven months of studying. However, the weight values of CH₄ for IDWr² and IDW-slope ranged between 0.0013 to 0.69 and 0.0439 to 0.5713, respectively, for the seven months of studying. Whereas the weight values for O₃ of IDWr² and IDW-slope ranged between 0.06 to 0.33 and 0.1669 to 0.8007, respectively, in seven months.

Analyze satellite (remote sensing) measurements for CO_2 , CH_4 , and O_3 GHGs. Carbon dioxide (CO_2)

The satellite (RS) measurements of CO₂ by Orbiting Carbon Observatory-2 (OCO-2), which is an Earth observing satellite and Launched on July 2, 2014. It must be pointed out that OCO-2 completes an orbit in 98.8 min, and it has a set of about 233 orbit paths that repeat in 16-day cycles. The spatial

resolution of OCO-2 at nadir is around 1.3 x 2.25 km (4). For that reason, the observed CO₂ concentrations were 416, 417, and 418 ppm along all the studied locations for Dec./21, Jan./22, and Feb./22, respectively, due to its low spatial resolution of the satellite and all the locations were positioned within one pixel. Additionally, the satellite provided CO₂ date till February 28, 2022, thus, we couldn't obtain CO₂ concentration data for remaining of scheduled months. Our results of CO₂ emission agree to some extent with Eldering, Wennberg (10) findings for atmospheric Carbon dioxide concentration, which is currently about 400 ppm due to inequity between CO₂ emissions and removal, and then an increase of 2 to 3 ppm will occur per year. Moreover, a quarter of CO₂ emitted by anthropogenic activities is being absorbed by the ocean, then another quarter is absorbed by processes on land.

The RMSE values for CO₂ ranged between (45 to 92.75 ppm) on December 2021, but in January and February, 2022 were between (0.5 to 87 ppm) and (1.83 to 43.17 ppm) respectively, knowing that importance of RMSE values is to indicate how the absolute fit of model is to the observed data, or it shows how close the observed data points are to model's predicted values. Moreover, Lower values of RMSE indicate better fit. The RS measurement overestimated ground measurement at location 13 by (1.09 %). However, at the other 12 locations, RS measurements were underestimated of ground measurements in December 2021 and January 2022. Also, on February 2022, the RS measurements underestimated the ground measurement at locations 4, 8, 5, 6, and 2 by (-6.86, -6.76, -2.67, -0.59, and -0.43 %) respectively.

Methane (CH₄)

Regarding the RS measurement of CH₄ through the recognized satellite, unfortunately we were not able to obtain the satellite readings or images for all locations and during months of study because images were not delivered for all locations in study area, as it is shown in Table 4 and 5 as well in Figure 2. This can be due to fact that quality of formation or the digital image is characterized principally by its resolution. Thus, spatial resolution of an images is one of essential aspects of remote sensing, which is in turn determined by the number of pixels from which the image is composed of, but not always high resolution of digital image produced testifies its high quality. Also, the distance between object and satellite equipment's capabilities play its role for spatial resolution. Therefore, remote sensing can be performed at low, medium, and high spatial resolutions. High spatial resolution could be achieved close to surface ground this can capture images with exceptionally high spatial resolution (33). High resolution is often linked with high accuracy. Furthermore, clouds also play a vital role in filtering, obscuring, and in certain cases blocking the imagery satellites capture (37). Although optical remote sensing imagery characterizes by its high resolution and stable geometric properties and has been used widely in many

fields, remote sensing imagery is certainly affected by climate condition, particularly clouds. Therefore, eliminating the cloud in high-resolution remote sensing satellite image is an essential pre-processing phase before analyzing it. Consequently, neural networks have been successfully used in many image processing tasks to remove clouds in remote sensing, but imagery is still relatively small (32). In general, we did not notice a particular trend for RS measurements of CH₄ along location as well as among months of study by satellite (Table 4, Table 5, and Figure 2 and 3). However, all locations except L13 revealed RS measurements in July and ranged between 1897.5 to 1908.3 ppb at locations L11 and L9, respectively. Our results are close to global average which indicated by NOAA (31), and they were between 1891.6 to 1909.6 ppb for May 2021 peak and April 2022 peak, respectively. Moreover, at L7, L9, L10, and L11, RS measurements of CH₄ were occurred at some locations as well as for some months and as follows: L7 (Feb, June, and July/22); L9 (Jan, Jun, and Jul/22); L10 (Dec./21, Jan., Apr., Jun., and July/22); and L11 (Dec./21, Jan., Jun., and July/22). Figures 2 shows the spatial distribution of CO₂, CH₄, and O₃ in January and February. It is worth noting that the range and level of concentration in case of remote sensing (RS) is narrower and less (1858.99 - 1908.26 ppb) compared to ground measurement, as shown (500.00 - 3880.95 ppb), and this may be attributed to fact that satellite measurements of GHGs provide a very large spatial coverage and measures of atmospheric whole column. Other consideration that should be stated, 23 RS measurements of methane gas were recorded only out of a total of 91 RS measurements, and of recorded measurements, 16 of them, i.e. (69.5%), appeared only in June and July 2022 only. Hence, no or limited RS data were obtained for CO2 and CH4 GHGs in some months and along studied locations, as shown in the Figure 2 and 3 as well as Table 5. This might be linked to seasonal climatic condition particularly relative temperature, solar radiation, and sky clear of clouds. The RS measurement overestimated ground measurement by (26.22 %) in Kelaspy, but in Bakrajo, the RS measurement underestimated the ground measurement by (-5.59 %). Additionally, the RS measurements overestimated the ground measurements in January and February 2022 at all points.

$Ozone(O_3)$

Although RS measurements of Ozone concentration were obtained for all studied locations and along all scheduled months, the variation in RS concentrations were ranged only between 15.13 to 17.75 ppb, that means, difference was only 2.62 ppb (Tables 4 and 5). This can be attributed to fact that attaining sensitivity to atmospheric structures troposphere creating and high vertical resolution profiles is a challenging issue for many satellite instruments due to previous mentioned reasons on comparing between ground and satellite measurements, and that is why a significant variation for ground measurements were revealed and ranged between 0.25 to 64 ppb with a difference concentration level of 63.75 ppb. In general, we did not notice a particular trend for RS measurements of O₃ concentrations along the location as well as among months of study by RS measurements (Table 4, Table 5, and Figure 2 and 3). Conversely, an increasing trend of O₃ concentrations were observed generally by all locations from December/21 to March/22, owing to lengthening of the daytime and increasing the temperature. Generally, O₃ concentrations is positively correlated with temperature and solar radiation intensity (21).Additionally, the measurements underestimated the ground measurements in Kelaspy, Tanjaro, and Hawareshar park by (-29.31, -25.98, and -3.18 %), respectively. It is worth noting that concentration of O₃ decreases at night and in early morning hours because of a lack of reactions, it increases during the daytime because of increased solar irradiation, which encourages the creation of O_3 through photochemical reactions in lower troposphere (19). From the above-mentioned results, we can conclude in this study that no observable compatibility was recognized between the ground and satellite measurements regarding the designated locations for the range's limits of the studied GHGs of Carbon dioxide, Methane, and Ozone during scheduled months.

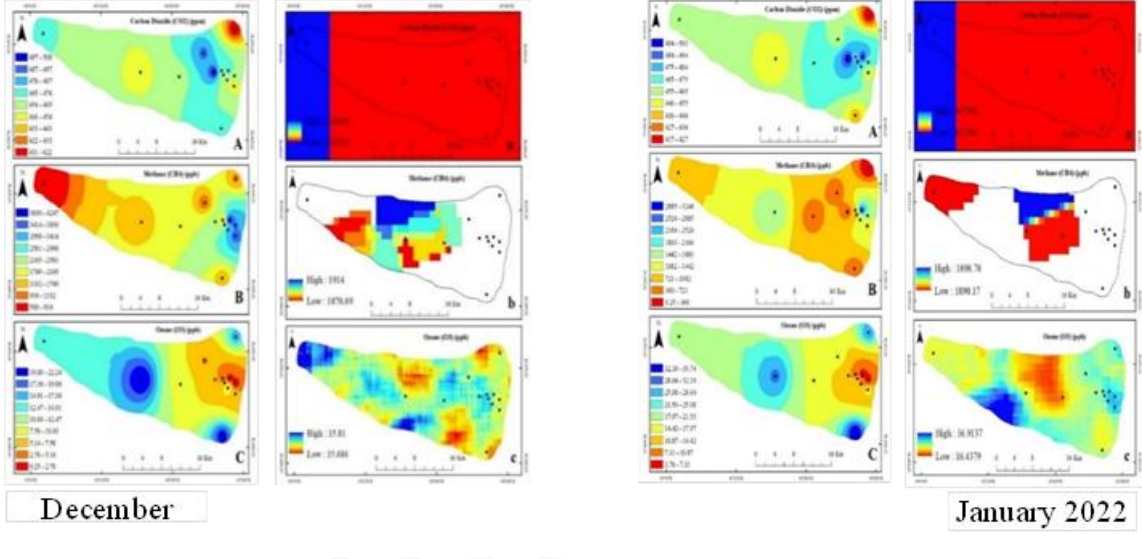
This could be explained bv satellite photographs showing greenhouse gases across the atmosphere. The actual concentration of greenhouse gases in satellite image may be above the earth's surface. kilometers Therefore, it is essential to compare the ground measurements to the satellite measurements to find out that observed greenhouse gases by satellite images are on the ground surface. Also, because an image's level of detail depends on spatial resolution of satellite used, and the spatial resolution of images is one of essential aspects of remote sensing. reason is spatial resolution of satellite image, as in Orbiting Carbon Observatory-2 (OCO-2) satellite for measuring carbon dioxide has a low spatial resolution $(0.5^{\circ} \times 0.625^{\circ})$. Another reason is that no RS data was available for CO₂ during the study period, such as GOSAT and TanSat satellites.

Table 4. Statistical summary of ground and remote sensing measurements for CO₂, CH₄, and O₃ from December 2021 to July 2022

Location		December			January			February			March			April			June		July			
Numbers	Gases	RS	RMSE	PBIAS	RS	RMSE	PBIAS	RS	RMSE	PBIAS	RS	RMSE	PBIAS	RS	RMSE	PBIAS	RS	RMSE	PBIAS	RS	RMSE	PBIAS
	CO2	416	53.50	-11.40	417	50.5	-10.8	418	1.84	0.44	/	/	/	/	/	/	/	/	/	/	/	/
1	CH4	/	/	/	/	/	/	/	/	/	/	/	/	/	/	/	/	/	/	1900.04	1599.96	-45.71
	O3	15.75	13.25	530	16.65	6.9	70.76	16.31	7.02	-30.09	16.94	2.56	-13.12	16.85	9.85	140.71	15.42	2.83	-15.50	15.16	28.34	-65.14
	CO2	416	39.75	-8.72	417	69.25	-14.24	418	1.83	-0.43	/	/	/	/	/	/	/	/	/	/	/	/
2	CH4	/	/	/	/	/	/	/	/	/	/	/	/	/	/	/	/	/	/	1900.04	599.96	-23.99
	O3	15.75	9	133.33	16.64	3.64	28	16.33	16.17	-49.75	16.94	18.06	-51.6	16.86	6.14	-26.69	15.43	13.57	-46.79	15.17	10.33	-40.50
	CO2	416	33.5	-7.45	417	51	-10.89	418	6.84	1.66	/	/	/	/	/	/	/	/	/	/	/	/
3	CH4	/	/	/	/	/	/	/	/	/	/	/	/	/	/	/	/	/	/	1900.04	1599.96	-45.71
	O3	15.75	3.25	26	16.7	5.7	51.81	16.33	16.17	-49.75	16.93	20.07	-54.24	16.86	16.14	-48.90	15.43	9.32	-37.65	15.18	10.32	-40.47
	CO2	416	59	-12.42	417	83.5	-16.68	418	30.83	-6.86	/	/	/	/	/	/	/	/	/	/	/	/
4	CH4	/	/	/	/	/	/	/	/	/	/	/	/	/	/	/	/	/	/	1906.95	2593.05	-57.62
	O3	15.73	14.98	1997.33	16.67	12.92	344.53	16.3	5.47	50.50	16.94	6.44	61.33	16.86	13.86	462	15.41	12.91	516.4	15.16	16.34	-51.87
	CO2	416	45.75	-9.9	417	50.75	-10.84	418	11.5	-2.67	/	/	/	/	/	/	/	/	/	/	/	/
5	CH4	/	/	/	/	/	/	/	/	/	/	/	/	/	/	/	/	/	/	1906.95	2093.05	-52.32
	O3	15.73	15.48	6192	16.67	11.92	250.94	16.28	5.28	48	16.94	2.44	16.82	16.86	4.86	40.5	15.42	3.42	28.5	15.15	1.85	-10.88
	CO2	416	30.25	-6.77	417	26.25	-5.92	418	2.5	-0.59	/	/	/	/	/	/	/	/	/	/	/	/
6	CH4	/	/	/	/	/	/	/	/	/	/	/	/	/	/	/	/	/	/	1906.95	1593.05	-45.51
	O3	15.72	9.72	162	16.67	0.08	-0.47	16.33	1.33	8.86	16.93	4.93	41.08	16.87	0.87	5.43	15.41	6.66	76.11	15.17	5.83	-27.76
	CO2	416	56.25	-11.91	417	25.5	-5.76	418	10.17	2.49	/	/	/	/	/	/	/	/	/	/	/	/
7	CH4	/	/	/	/	/	/	1883.27	883.27	88.32	/	/	/	/	/	/	1858.99	1108.99	147.86	1907.16	2592.84	-57.61
	O3	15.72	5.53	-26.02	16.58	19.17	-53.62	16.4	21.26	-56.45	16.88	21.62	-56.15	16.87	28.13	-62.51	15.45	14.3	-48.06	15.19	22.81	-60.02
	CO2	416	92.75	-18.23	417	87	-17.26	418	30.33	-6.76	/	/	/	/	/	/	/	/	/	/	/	/
8	CH4	/	/	/	/	/	/	/	/	/	/	/	/	/	/	/	/	/	/	1900.04	1599.96	-45.71
	O3	15.76	9.76	162.66	16.61	5.61	51	16.33	2	-10.91	16.94	9.56	-36.07	16.84	15.84	1584	15.44	16.06	-50.98	15.16	9.34	-38.12
	CO2	416	50	-10.72	418	40.33	-8.79	418	8.17	1.99	/	/	/	/	/	/	/	/	/	/	/	/
9	CH4	/	/	/	1890.17	890.17	89.01	/	/	/	/	/	/	/	/	/	1884.01	1384.01	276.80	1908.26	1091.74	-36.39
	O3	15.79	1.29	8.89	16.57	2.18	-11.62	16.67	17.16	-50.72	16.96	34.04	-66.74	16.9	3.1	-15.5	15.41	34.59	-69.18	15.14	34.36	-69.41
	CO2	416	31.75	-7.09	417	29.75	-6.65	418	23	5.82	/	/	/	/	/	/	/	/	/	/	/	/
10	CH4	1893.37	393.37	26.22	1893.92	143.92	8.22	/	/	/	/	/	/	1897.02	897.02	89.70	1886.57	886.57	88.65	1901.56	598.44	-23.93
	O3	15.72	6.53	-29.34	16.56	12.69	-43.38	16.15	28.18	-63.56	16.95	36.05	-68.01	16.86	24.14	-58.87	15.43	43.07	-73.62	15.17	45.83	-75.13
	CO2	416	43.25	-9.41	417	51	-10.89	418	2.34	0.56	/	/	/	/	/	/	/	/	/	/	/	/
11	CH4	1888.07	111.93	-5.59	1893.92	1393.92	278.78	/	/	/	/	/	/	/	/	/	1874.85	624.85	49.98	1897.45	102.55	-5.12
	O3	15.74	6.24	65.68	16.48	1.52	-8.44	16.24	14.26	-46.75	16.94	14.56	-46.22	16.84	9.16	-35.23	15.43	16.57	-51.78	15.17	15.33	-50.26
	CO2	416	75.25	-15.31	417	41.25	-9	418	19.5	4.89	/	/	/	/	/	/	/	/	/	/	/	/
12	CH4	/	/	/	/	/	/	/	/	/	/	/	/	/	/	/	/	/	/	1900.89	99.11	-4.95
	O3	15.73	10.73	214.6	16.63	1.12	-6.30	16.27	11.89	-42.22	16.96	20.54	-54.77	16.83	19.17	-53.25	15.41	24.34	-61.23	15.16	20.84	-57.88
	CO2	416	4.5	1.09	417	0.5	-0.11	418	43.17	11.51	/	/	/	/	/	/	/	/	/	/	/	/
13	CH4	/	/	/	/	/	/	/	/	/	/	/	/	/	/	/	/	/	/	/	/	/
	O3	15.73	0.52	-3.2	16.64	11.86	-41.61	16.23	19.93	-55.11	16.94	43.06	-71.76	16.86	37.14	-68.77	15.41	30.84	-66.68	15.13	48.87	-76.35

Table 5. Measured concentration ranges of ${\rm CO_2}, {\rm CH_4},$ and ${\rm O_3}$ from ground measurements and remote sensing

LoNo.	The months	GHG	Ranges of ground measure.	Appearance sites of the ranges	Ranges of Remote Sensing or Satellite extracted data	Appearance sites of the ranges	The possibility measurement of CC and CH4 via RS were only at the aforementioned below locations
		CO2	411.5-508.8	L13 – L8	416-416	Concentration was the same	At all locations
1	Dec./21	CH4	500-4250	L9 – L4	1888.1-1893.4	L11-L10	At L10 and L11
		O3	0.25-22.25	L5 - L10	15.72-15.79	L6, L7, L10- L1, L2, L3	NM
		CO ₂	417.5-504.0	L13 – L8	417-418	at all locations except L9 - only at L9 was 418	At all locations
2	Jan./22	CH_4	0.0-3250	L13 – L4	1890.2- 1893.9	L9- L10, L11	At L9, L10 and L11
		O_3	3.75-35.75	L4 - L7	16.48- 16.70	L11- L4, L5, L6	NM
		CO2	374.8-448.8	L13 – L4,8	418- 418	Concentration was the same	At all locations
3	Feb./22	CH4	0.0- 2666.7	L13 – L4	1883.3	L7	Only L7
		03	10.83-44.33	L4 - L10	16.15- 16.67	L10- L9	NM
		CO2	337.5-377.0	L13 – L5	Not measured		At all locations
4	Mar./22	CH4	0.0-3000	L8,9,10,13- L4	Not measured		At all locations
		O3	10.5- 60.0	L4 – L13	16.88- 16.96	L7 – L12	NM
		CO ₂	285.0-408.0	L13 – L8	Not measured		At all locations
5	Apr./22	CH4	0.0- 17000	L6,7,11,12,13- L1	1897	L10	Only L10
		03	1.0-54.0	L8 - L13	16.83-16.90	L12 – L9	NM
		CO2	427.8-491.8	L13- L4	Not measured		At all locations
6	Jun./22	CH4	500-3500	L3,9 -L5	1858.1-1886.6	L9-L11	L9, L10 and L11
		03	2.5- 58.5	L4- L10	15.41-15.45	L2, L3, L10, L11- L7	NM
		CO ₂	430- 466	L13- L2	Not measured		At all locations
7	July./22	CH4	500-4500	L13, 9- L 4, 7	1897.5- 1908.3	L11-L9	At all locations except L13
		03	17-64	L5- L13	15.13-15-19	L13- L7	NM
	concentration ring the mont	unites:	ppm for CO2 and p			L13-L7 means ozone measurements by the	



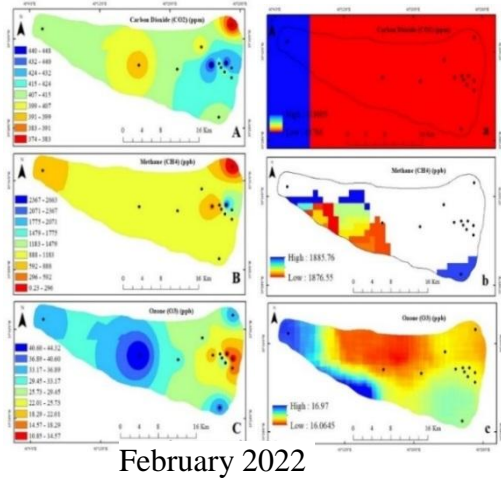


Figure 2. Spatial distributions of greenhouse gases (CO_2) , (CH_4) , and (O_3) concentrations in (ppm, ppb) and during the study period (Maps A, B, and C indicate ground measurements for 13 locations, while a, b, and c represent satellite map)

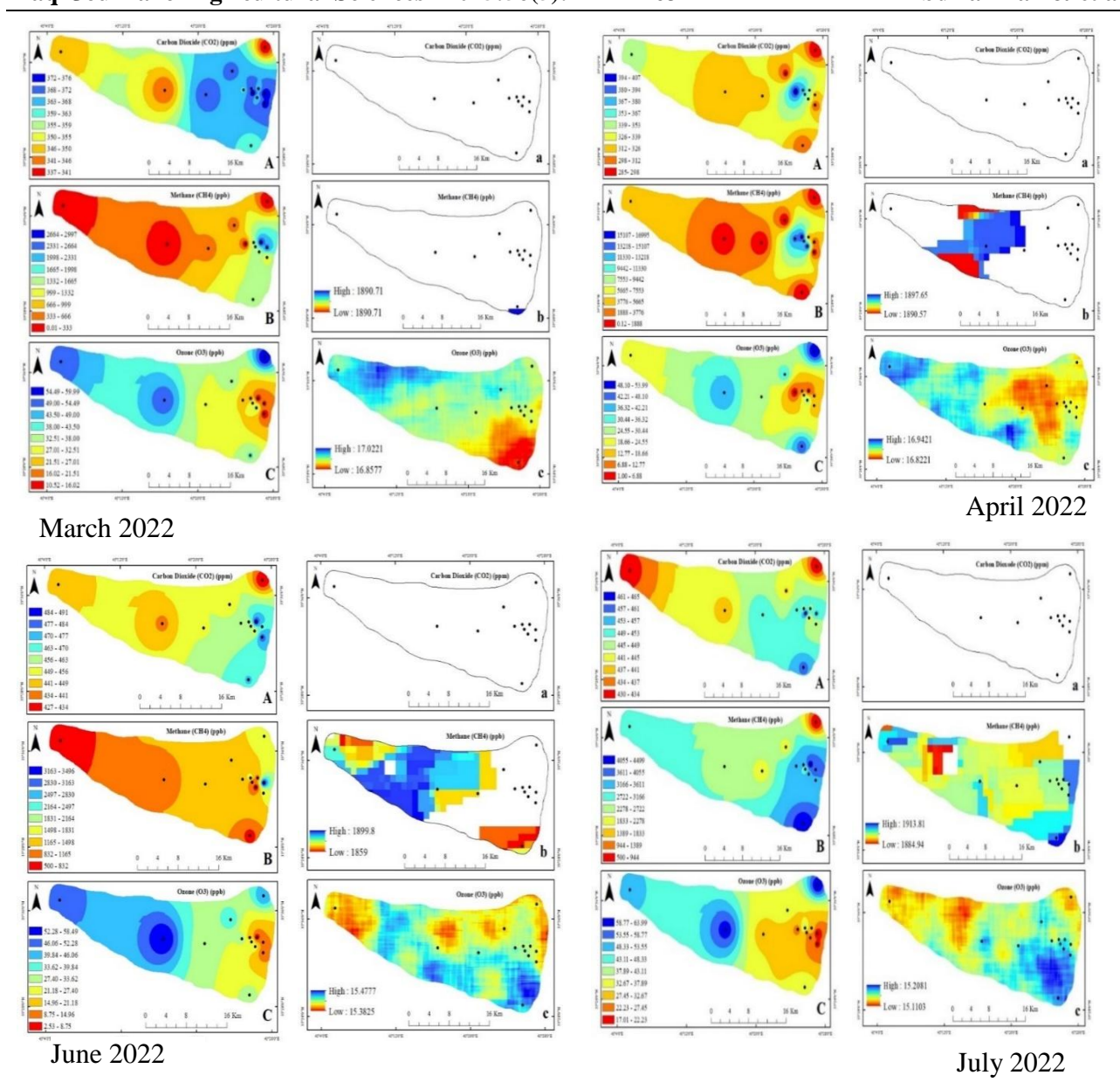


Figure 3. Spatial distributions of greenhouse gases (CO₂), (CH₄), (O₃) concentrations in (ppm, ppb and during the study period (Maps A, B, and C indicate ground measurements for 13 points, while a, b, and c represent satellite maps)

CONCLUSION

In this study, we used for first time Sentinel 5 Precursor TROPOMI (S5P) and Orbiting Observatory-2 (OCO-2) Carbon satellite images as well as ground measurements datasets from December 2021 to July 2022 to analyze the spatial-temporal distribution of CO₂, CH₄, and O₃ GHGs at 13 locations in Sulaimani city, KR, Iraq, because GHGs are currently a global concern, and continue to increase due to anthropogenic factors, then this is followed by global warming and climate change. However, it should be point out that our study faced limitations of lack of previous research studies about GHGs issue, there are no air quality monitoring stations in Sulaimani

city, and the researchers have no access to some real-time and highest resolution satellite imagery. Accordingly, further more remote sensing study and ground investigation are required to determine the local concentration of GHGs and also to study the effects of climate change on the air quality at Sulaimani City. In this study, ground measurements of concentrations for CO₂, CH₄, and O₃ GHGs noticeable showed and significant differences for studied gases within the study locations as well as over months of study. Although satellite measurements for ozone gas were obtained at all studied locations and for all months, the differences between the tempospatial measurements were very limited and not significant due to the lack of sensitivity of used satellite. On the other hand, obtaining satellite reading for carbon dioxide gas was only for limited months because the satellite measuring record for CO₂ was till February 28, 2022. Furthermore, the range of temporal and spatial differences of CO2 were also not significant by the satellite measurements due to the lack of the sensitivity for the satellite used or relied upon in this study. Also, with regard to satellite measuring of methane gas concentration, we were unable to obtain readings for all locations and months of the study, and spatial and temporal differences were also limited and not significant. This could be attributed to fact that satellite-based remote sensing has certain limitations in terms of spatial and temporal resolution of the data. Local cloudiness, low temporal and spatial resolution, and gaps on image create a case for atmospheric complex measurements. Additionally, spatial resolution of satellite image, as in Orbiting Carbon Observatory-2 (OCO-2) satellite for measuring Carbon dioxide, has a low spatial resolution $(0.5^{\circ} \times 0.625^{\circ})$. Further reason is no remote sensing (RS) data was available for CO2 during the study period, such as by GOSAT and TanSat satellites. Therefore, improvement in spatial resolution could improve the estimation accuracy of CO₂, CH₄, and O₃ concentrations from satellites measurements. It is worth mentioning in conclusion also that climatic factors such as; relative humidity, temperature, pressure, humidity, and wind should be regarded in GHGs measurements because they are dynamic factors that impact measurements of them.

CONFLICT OF INTEREST

The authors declare that they have no conflicts of interest.

DECLARATION OF FUND

The authors declare that they have not received a fund.

REFERENCES

- 1. Al-Madi, A. M. and M. L. Maina. 2013. The role of GIS and remote sensing in mapping the distribution of greenhouse gases. European Sci. J. 9 (36):404-410
- 2. Al-Taay, M. S. A., A. H. A. Al-Assie and R. O. Rasheed. 2018. Impact of bazian cement factory on air, water, soil, and some green

plants in Sulaimani city-Iraq. Iraqi J. Agric. Sci. 49 (3):463-477. https://doi.org/10.36103/ijas.v49i3.118

- 3. America's Children and the Environment 2015. Criteria air pollutants. Third Edition. p.1-5.
- 4. An, N., F. Mustafa, L. Bu, M. Xu, Q. Wang, M. Shahzaman, M. Bilal, S. Ullah and Z. Feng. 2022. Monitoring of atmospheric carbon dioxide over Pakistan using satellite dataset. Remote Sens. 14 (5882):1-19. https://doi.org/10.3390/rs14225882
- 5. Breon, F.-M. and P. Ciais. 2010. Spaceborne remote sensing of greenhouse gas concentrations. C. R. Geoscience. 342 (4-5):412-424. DOI: 10.1016/j.crte.2009.09.012 6. Chen, B., X. Yang and J. Xu. 2022. Spatiotemporal variation and influencing factors of ozone pollution in Beijing. Atmosphere. 13

https://doi.org/10.3390/atmos13020359

(359):1-15.

7. Ciais, P., J. Tan, X. Wang, C. Roedenbeck, F. Chevallier, S.-L. Piao, R. Moriarty, G. Broquet, C. Le Quéré, J. G. Canadell, S. Peng, B. Poulter, Z. Liu and P. Tans. 2019. Five decades of northern land carbon uptake revealed by the interhemispheric CO₂ gradient. Nature. 568 (7751):221-225.

https://doi.org/10.1038/s41586-019-1078-6

- 8. Dewan, S. and A. Lakhani. 2022. Tropospheric ozone and its natural precursors impacted by climatic changes in emission and dynamics. Front. Environ. Sci. 10 (3389):1-21. https://doi.org/10.3389/fenvs.2022.1007942
- 9. Downie, R., J. Faris, H. Lam and L. Shirley. 2019. Estimation of carbon sequestration levels in trees for Canterbury plantings. 2019. Univ. Canterbury. Rep.p.17
- 10. Eldering, A., P. O. Wennberg, D. Crisp, D. S. Schimel, M. R. Gunson, A. Chatterjee, J. Liu, F. M. Schwandner, Y. Sun, C. W. O'dell, C. Frankenberg, T. Taylor, B. Fisher, G. B. Osterman, D. Wunch, J. Hakkarainen, J. Tamminen and B. Weir. 2017. The orbiting carbon observatory-2 early science investigations of regional carbon dioxide fluxes. Science. 358 (6360):1-8.

DOI: 10.1126/science.aam5745

11. EPA, Environmental Protection Agency. 2022. Importance of methane. Global methane initiative. Available at: https://www.epa.gov/gmi/importance methane.

- 12. Fitzky, A. C., H. Sandén, T. Karl, S. Fares, C. Calfapietra, R. Grote, A. Saunier and B. Rewald. 2019. The interplay between ozone and urban vegetation—BVOC emissions, ozone deposition, and tree ecophysiology. Front. For. Glob. Change. 2 (50):1-17. https://doi.org/10.3389/ffgc.2019.00050
- 13. Fletcher, S. E. M., P. P. Tans, L. M. Bruhwiler, J. B. Miller and M. Heimann. 2004. CH_4 sources estimated from atmospheric observations of CH_4 and its. Glob. Biog. Cycl. 18 (1):1-17.
- 14. Guo, H., M. F. Goodchild and A. Annoni, 2020. Manual of digital Earth. Sprin. Nature.p:1-849
- 15. Hansen, J., R. Ruedy, M. Sato and K. Lo. 2010. Global surface temperature change. Rev. Geophys. 48 (4):1-29
- 16. Hardwick, S. and H. Graven. 2016. Satellite observations to support monitoring of greenhouse gas emissions. Granth. Instit. 16:2-16
- 17. IPCC, Intergovernmental Panel on Climate Change. 2013. Climate change 2013: The physical science basis contribution of working group I to the fifth assessment report of the intergovernmental panel on climate change. Cambridge Univ. Press.
- 18. IPCC, Intergovernmental Panel on Climate Change. 2017. IPCC fourth assessment report: climate change 2007: working group I: the physical science basis TS.2.1greenhouse. Gaseshttps://archive.ipcc.ch/publications_and_data/ar4/wg1/en/tssts-2-1.html.
- 19. Kasparoglu, S., S. Incecik and S. Topcu. 2018. Spatial and temporal variation of O_3 , NO and NO_2 concentrations at rural and urban sites in Marmara Region of Turkey. Atmos. Pollut. Res. 9 (6):1009-1020.

https://doi.org/10.1016/j.apr.2018.03.005

20. Kinney, P. L. 2018. Interactions of climate change, air pollution, and human health. Curr. Envir. Health Rpt. p.5. 179–186.

https://doi.org/10.1007/s40572-018-0188-x

21. Lacour, S. A., M. De Monte, P. Diot, J. Brocca, N. Veron, P. Colin and V. Leblond. 2006. Relationship between ozone and temperature during the 2003 heat wave in France: consequences for health data analysis. BMC. Pub. Health. 6 (1):1-8.

https://doi.org/10.1186/1471-2458-6-26

- 22. Li, K., D. J. Jacob, L. Shen, X. Lu, I. De Smedt and H. Liao. 2020. Increases in surface ozone pollution in China from 2013 to 2019: anthropogenic and meteorological influences. Atmos. Chem. Phys. 20 (9):11423-11433. https://doi.org/10.5194/acp-20-11423-2020
- 23. Li, S., Y. W. Siu and G. Zhao. 2021. Driving factors of CO_2 emissions: further study based on machine learning. Front. Environ. Sci. 323 (9):1-16.

https://doi.org/10.3389/fenvs.2021.721517

24. Lopez, M., M. Schmidt, M. Ramonet, J.-L. Bonne, A. Colomb, V. Kazan, P. Laj and J.-M. Pichon. 2015. Three years of semicontinuous greenhouse gas measurements at the Puy de Dôme station (central France). Atmo. Measu. Techn. 8 (9):3941-3958.

https://doi.org/10.5194/amt-8-3941-2015

- 25. Mahal, S. H., A. M. Al-Lami and F. K. Mashee. 2022. Assessment of the impact of urbanization growth on the climate of Baghdad province using remote sensing techniques. Iraqi J. Agric. Sci. 53 (5):1021-1034. https://doi.org/10.36103/ijas.v53i5.1616
- 26. Majid, S. N. 2011. Valuation of ambient air pollution: a study of some urban areas in Sulaimani city and its surrounding/Kurdistan region of Iraq. Univer. Sulaimani. p.277
- 27. Mirzaei, R. and M. Sakizadeh. 2016. Comparison of interpolation methods for the estimation of groundwater contamination in Andimeshk-Shush Plain, Southwest of Iran. Envir. Sci. Pollut. Res. 23 (3):2758-2769. https://doi.org/10.1007/s11356-015-5507-2
- 28. Mohammed, Y. H., S. N. Majid and P. M. Najmaddin. 2022. Ambient particulate matter concentrations for difference size from MODIS satellite images and ground measurements in Sulaimani, Iraq. Appli. Ecolo. Envir. Sci.10 (10):622-639
- 29. Najmaddin, P. M., N. B. Salih and T. A. Abdalla. 2020. Evaluating the spatial distribution of some soil geotechnical properties using various interpolation methods (case study: Sulaimani province, Iraq). J. Soil Sci. Agric. Eng. 11 (7):275-281
- 30. Najmaddin, P. M., M. J. Whelan and H. Balzter. 2017. Application of satellite-based precipitation estimates to rainfall-runoff modelling in a data-scarce semi-arid catchment. Climate. 5 (32):1-22.

https://doi.org/10.3390/cli5020032

- 31. NOAA, National Oceanic and Atmospheric Administration. 2022. Trends in atmospheric carbon dioxide; Maunaa Loa CO₂ record. U.S. Department of commerce, global monitoring division. Available at: https://gml.noaa.gov/ccgg/trends/.
- 32. Pan, H. 2020. Cloud removal for remote sensing imagery via spatial attention generative adversarial network. ArXiv. abs/2009.13015:1-7.

https://doi.org/10.48550/arXiv.2009.13015

33. Prudyus, I., V. Tkachenko, P. Kondratov, S. Fabirovskyy, L. Lazko and A. Hryvachevskyi. 2015. Factors affecting the quality of formation and resolution of images in remote sensing systems. Compu. Pro. Elec. Eng. 5 (1):41-46.

http://nbuv.gov.ua/UJRN/CPoee 2015 5 1 1 0

- 34. Ravishankara, A. R., J. S. Daniel and R. W. Portmann. 2009. Nitrous oxide (N_2O): the dominant ozone-depleting substance emitted in the 21st century. Science. 326 (5949):123-125. DOI: 10.1126/science.1176985
- 35. Reynolds, R. F., W. L. Bauerle and Y. Wang. 2009. Simulating carbon dioxide exchange rates of deciduous tree species: evidence for a general pattern in biochemical changes and water stress response. Anna. Bot. 104 (4):775-784.

https://doi.org/10.1093/aob/mcp156

36. Rigby, M., R. G. Prinn, S. O'doherty, B. R. Miller, D. Ivy, J. Mühle, C. M. Harth, P. K.

- Salameh, T. Arnold, R. F. Weiss, P. B. Krummel, L. P. Steele, P. J. Fraser, D. Young and P. G. Simmonds. 2014. Recent and future trends in synthetic greenhouse gas radiative forcing. Geophys. Res. Lett. 41 (7):2623-2630. https://doi.org/10.1002/2013GL059099
- 37. Robinson, T. R., N. Rosser and R. J. Walters. 2019. The spatial and temporal influence of cloud cover on satellite-based emergency mapping of earthquake disasters. Sci. Rep. 9 (1):1-9.

https://doi.org/10.1038/s41598-019-49008-0

38. Sarangi, T., M. Naja, N. Ojha, R. Kumar, S. Lal, S. Venkataramani, A. Kumar, R. Sagar and H. C. Chandola. 2014. First simultaneous measurements of ozone, CO, and NOy at a high-altitude regional representative site in the central Himalayas. J. Geophys. Res. Atmos. 119 (3):1592-1611.

https://doi.org/10.1002/2013JD020631

39. Sekiya, T. and K. Sudo. 2012. Role of meteorological variability in global tropospheric ozone during 1970–2008. J. Geophys. Res. 117 (D18):1-16.

https://doi.org/10.1029/2012JD018054

40. Sillman, S. 1999. The relation between ozone, NOx and hydrocarbons in urban and polluted rural environments. Atmos. Envir. 33 (12):1821-1845.

https://doi.org/10.1016/S1352-2310(98)00345-8

41. Sulaymaniyah Governorate Profile 2015. Sulaymaniyah governorate profile – NCCI.